Title
Human Responses to Visually Evoked Threat

Journal
Current Biology, 31(3)

ISSN
0960-9822

Authors
Yilmaz Balban, Melis
Cafaro, Erin
Saue-Fletcher, Lauren
et al.

Publication Date
2021-02-01

DOI
10.1016/j.cub.2020.11.035

Peer reviewed

HHS Public Access

Author manuscript

Curr Biol. Author manuscript; available in PMC 2021 August 31.

Published in final edited form as:

Curr Biol. 2021 February 08; 31(3): 601–612.e3. doi:10.1016/j.cub.2020.11.035.

Human Responses to Visually Evoked Threat

Melis Yilmaz Balban[1], **Erin Cafaro**[1], **Lauren Saue-Fletcher**[1], **Marlon J. Washington**[1], **Maryam Bijanzadeh**[4], **A. Moses Lee**[4], **Edward F. Chang**[4], **Andrew D. Huberman**[1,2,3,5,*]

[1]Department of Neurobiology, Stanford University School of Medicine, Stanford, CA 94305, USA

[2]Department of Ophthalmology, Stanford University School of Medicine, Stanford, CA 94305, USA

[3]BioX, Stanford University School of Medicine, Stanford, CA 94305, USA

[4]Department of Neurological Surgery, University of California, San Francisco, 400 Parnassus Avenue, San Francisco, CA 94143, USA

[5]Lead Contact

SUMMARY

Vision is the primary sense humans use to evaluate and respond to threats. Understanding the biological underpinnings of the human threat response has been hindered by lack of realistic in-lab threat paradigms. We established an immersive virtual reality (VR) platform to simultaneously measure behavior, physiological state, and neural activity from the human brain using chronically implanted electrodes. Subjects with high anxiety showed increased visual scanning in response to threats as compared to healthy controls. In both healthy and anxious subjects, the amount of scanning behavior correlated with the magnitude of physiological arousal, suggesting that visual scanning behavior is directly linked to internal state. Intracranial electroencephalography (iEEG) recordings from three subjects suggested that high-frequency gamma activity in the insula positively correlates with physiological arousal induced by visual threats and that low-frequency theta activity in the orbitofrontal cortex (OFC) negatively correlates with physiological arousal induced by visual threats. These findings reveal a key role of eye movements and suggest that distinct insula and OFC activation dynamics may be important for detecting and adjusting human stress in response to visually perceived threats.

In Brief

Yilmaz Balban et al. investigate human responses to visual threats using behavioral, physiological, and neural recordings. They demonstrate that exposure to virtual heights triggers visual scanning

*Correspondence: adh1@stanford.edu.

AUTHOR CONTRIBUTIONS

Conceptualization, M.Y.B. and A.D.H.; Methodology, M.Y.B. and A.D.H.; Software, M.Y.B., M.B., and A.M.L.; Formal Analysis, M.Y.B., L.S.-F., M.B., and A.M.L.; Investigation, M.Y.B., A.D.H., E.C., M.J.W., and M.B.; Resources, M.B., A.M.L., E.F.C., and A.D.H.; Writing – Original Draft, M.Y.B. and A.D.H.; Writing – Review & Editing, M.Y.B. and A.D.H.; Visualization, M.Y.B.; Supervision, E.F.C. and A.D.H.

DECLARATION OF INTERESTS

A.D.H. is on the *Current Biology* advisory board.

SUPPLEMENTAL INFORMATION

Supplemental Information can be found online at https://doi.org/10.1016/j.cub.2020.11.035.

behavior proportional to the autonomic arousal response. Insula and orbitofrontal cortex show significant correlations with visually driven arousal.

INTRODUCTION

An ability to adaptively respond to threats is fundamental for survival and quality of life. Altered timing or magnitude of threat responses is prominent in anxiety disorders including post-traumatic stress disorder (PTSD).[1–3] For humans, visual perception of threats is especially crucial. Visually evoked threat responses have been studied extensively in mice, which revealed that physiological arousal levels shape the specific defensive behaviors elicited. Several of the key brain areas involved in that process have been identified in mice.[4–6] By contrast, the interaction between physiological arousal and defensive behaviors in humans remains poorly understood. Knowledge of the underlying neural circuits is similarly lacking. Given that altered physiological arousal and threat perception are key features of many psychiatric disorders,[7–9] it is important to understand how humans respond to visual threats at the level of behavior, physiology, and underlying neural circuit dynamics.

There are several challenges to studying human threat responses in the laboratory. It is straightforward to create a visual stimulus that mice perceive and react to as a predator,[4,10] but it has proved difficult to create laboratory environments and stimuli to study equivalent processes in humans, in particular while measuring people's behavioral responses.[11] Traditionally, laboratory studies of human fear and threat have relied on mental imagery, video games,[12,13] or still images.[14,15] Important insights between rodents and humans have emerged from those studies.[16,17] Most formats used for the human studies, however, were ineffective at triggering natural behavioral responses. In part that was due to the fact that (1) human subjects are aware that the threat stimuli are not real and (2) monitoring of physiological signals from humans in real time as they encounter threats was not technically feasible. As a consequence, most studies relied on self-report or other proxies of threat-induced and stress-induced behavior such as button clicks or post hoc surveys. Actual human behavioral responses to threats captured in real time have yet to be studied in mechanistic fashion in the laboratory.[12,16–18] Self-report studies that explore hypothetical threat responses are similarly hindered by the fact that people's reported responses might differ from their actual responses.[19] Thus, paradigms that evoke and measure real behaviors and physiological arousal in response to realistic threat stimuli are needed to study the connection between arousal and behavior and the underlying neural circuitry.[20,21] Here we designed an experimental platform that allowed us to achieve these goals.

RESULTS

Virtual Heights Reliably Trigger Physiological Arousal and Visual Scanning in Healthy Humans

We created a virtual reality (VR)-based paradigm to measure human behavioral and physiological responses to visual threats. VR allows subjects to feel deeply immersed in simulated environments and experience them as if they were real.[22,23] VR has been used effectively for exposure therapy to treat PTSD and phobias, thus validating its effectiveness

to activate the threat-processing circuitry in the brain.[24–26] To identify a visual stimulus that would reliably trigger physiological and behavioral responses, we created a virtual environment that starts as a mimic of the subject in an actual laboratory room (Figure 1A), then transitions to a series of potentially threatening stimuli such as swimming with great white sharks, being attacked by a dog, encountering a large spider, or exposure to heights (STAR Methods). While exposure to sharks, dogs, or spiders all evoked physiological responses (data not shown), the 3D simulation of heights consistently emerged as the visual stimulus that most reliably evoked robust physiological and behavioral responses (Video S1).

In order to create a sense of "immersion," which is a subject's realistic sense of being present in the virtual environment,[23] the heights exposure was introduced unexpectedly in the middle of a task subjects were instructed to perform (Figures 1B and 1C; Video S1). The task, called "lights-out," is a cognitive task that requires focused concentration on an external visual stimulus and executive functioning (STAR Methods). One minute into the task, the light board moved to the opposite end of the (virtual) room and subjects were exposed to the sudden appearance of a narrow, 150 ft-high-over-the-ground plank directly in front of them, and were instructed to cross the plank in order to continue the cognitive task (Figure 1C). The sudden appearance of the plank and the directions to cross were designed to trigger forced visual threat responses.

We measured subjects' physiological and natural behavioral responses before and during the height exposure as well as their subjective rating of their fear. Heart rate, respiration, and skin conductance level (SCL) were analyzed in healthy subjects (STAR Methods; Table S1) 10 s before introduction of the heights stimulus and during the sight of heights, but before subjects took their first step onto the plank. Subjects did not have any translational body motion at this time; therefore, the physiological and behavioral changes observed are only due to the exposure to the visual stimulus. In total, 38 out of 40 healthy subjects showed an increase in SCL upon seeing heights but before stepping onto the plank (Figures 1D and 1E; mean [Z score] ± SEM = 7.45 ± 1.31, $p < 0.0001$; see STAR Methods and Table S2 for all statistical details). In total, 28 out of 35 subjects exhibited an increase in heart rate, and six subjects had a decrease in heart rate (bradycardia). One subject exhibited no change in heart rate upon seeing heights (Figures 1D and 1F; mean change in heart rate [Z score] ± SEM = 0.84 ± 0.23, $p = 0.0077$). In total, 28 out of 34 subjects had an increase in tidal breath volume in response to heights, which reflected them holding their breath, a typical stress response (Figures 1D and 1G; mean [a.u.] ± SEM = 5.59 ± 1.53, $p = 0.0009$). These findings verify that the virtual heights stimulus was effective in triggering robust physiological arousal as all these measures, including bradycardia, indicate increased sympathetic nervous system activation.

Next, we assessed the subjects' behavioral responses to heights. Healthy subjects scanned the visual environment surrounding the plank before stepping onto it (Figures 1H and 1I; Video S1). To quantify this, we extracted gaze position from a VR-embedded eye-tracker that is the 3D coordinate (x, y, z) of the subject's point of gaze in virtual space (Figures 1H and 1I; STAR Methods). We defined a visual scanning episode as the time where gaze velocity exceeded 0.2 m/s for a period longer than 0.5 s (Figure 1J, top). This threshold

best matched manual assessment of subjects' visual scanning from videos. Healthy subjects showed, on average, 2.6 visual scans before stepping onto the plank (Figure 1J, bottom; mean ± SEM = 2.65 ± 0.33). Average scan distance was 1.57 m (Figure 1K; 1.57 ± 0.13 m [SEM]). We then analyzed whether each subjects' scanning behavior was related their level of physiological arousal in response to heights. There was a significant correlation between visual scanning and SCL responses to heights (Figure 1L; $rho_{spearman} = 0.43$, $p = 0.02$), indicating that visual scanning is reflective of and linked to physiological arousal.

Neutral "No Heights" Stimuli Do Not Trigger Visual Scanning or High Physiological Arousal

We tested whether the increases in physiological arousal and visual scanning were triggered directly by the simulated visual threat, e.g., heights, or alternatively, by the mere introduction of ambiguity in the visual environment. We introduced the sudden appearance of a "no heights" stimulus identical to the heights experience in every way except that subjects didn't encounter heights. Subjects were instructed to walk across the room after the walls and the ceiling were removed (Figures 2A and 2B; STAR Methods). The "no heights" stimulus evoked significantly less increase in SCL compared to heights (Figures 2C and 2D; mean change in SCL [Z score] ± SEM = 7.45 ± 1.30 and 1.85 ± 0.35, for heights and no heights, respectively; $p < 0.0001$). Response duration (quantified as width at half max of skin conductance responses [SCRs]) was also significantly shorter in "no heights" stimulus-exposed subjects compared to heights stimulus-exposed subjects (Figures 2D and 2E; mean ± SEM = 20.78 ± 2.46 s and 8.76 ± 0.88 s, for heights and no heights, respectively; $p < 0.0001$).

Surprisingly, changes in heart rate and respiration volume were not different in heights versus "no heights" (mean change in heart rate [Z score] ± SEM = 0.84 ± 0.30 and 0.43 ± 0.22, $p = 0.54$; mean change in tidal volume [a.u.] ± SEM = 5.59 ± 1.55 and 5.01 ± 0.91, $p = 0.76$, for heights and no heights, respectively). This suggests that skin conductance is the most sensitive measure of the visual threat response, whereas heart rate and respiration are more correlated with shifts in novelty of the visual environment. Since SCL changes were the most threat-sensitive response, we used SCL as an output of physiological arousal for the remainder of the study. The significantly lower SCL change in "no heights" compared to heights suggests that physiological arousal in response to heights is a threat response rather than a general saliency response.

Is visual scanning behavior different in response to the "no heights" compared to heights? The "no heights" stimulus triggered significantly less scanning than heights, as quantified by the total distance covered by scanning and the number of visual scans (Figures 2F and 2G; mean ± SEM = 3.64 ± 0.84 and 7.42 ± 1.09 for no heights versus heights, respectively; $p = 0.00061$). Neither distance covered by each scan nor frequency of scanning was significantly different (Figure 2H; data not shown; mean ± SEM = 1.65 ± 0.19 m and 1.57 ± 0.13 m, for no heights versus heights, respectively; $p = 0.73$). That subjects displayed greater visual scanning in response to the heights stimulus versus the control "no heights" stimulus condition indicates visual scanning is a threat response as opposed to simply exploratory behavior.[27,28] Subjects also rated the heights stimulus significantly scarier but no more

"real" than the "no heights" stimulus (Figure 2I; scary rating [out of 5], mean ± SEM = 2.18 ± 0.12 and 3.23 ± 0.18; real rating [out of 5], mean ± SEM = 3.29 ± 0.15 and 3.26 ± 0.13, for no heights versus heights, respectively; $p < 0.0001$ [scary], $p = 0.75$ [real]). The scary and real ratings for both heights and "no heights" stimuli were not correlated ($rho_{spearman} = 0.16$ and 0.13, $p = 0.42$ and 0.33, for heights versus no heights, respectively), suggesting how "scary" subjects perceived the stimuli was independent of their sense of immersion in VR.

Behavioral inhibition is a core feature of anxiety.[18,29–31] It is unknown, however, whether fear responses to visual threats as opposed to generalized anxiety also inhibit goal-directed behavior. Thus, we asked whether the heights stimulus inhibited approach toward a goal as compared to the "no heights" stimulus. The specified goal in the context of the heights paradigm was for subjects to score maximum points on the cognitive task, and this required subjects to cross the plank. In order to quantify suppression of approach, we measured subjects' latency to step onto the plank after the first sight of heights, or in case of the control condition, the latency to step toward the opposite side of the room in the "no heights" environment. Average latency to step onto the plank after the sight of heights was 6.1 s, significantly longer than the latency to the first step in the "no heights" condition (Figure 2J; mean ± SEM = 2.31 ± 0.20 s and 6.34 ± 0.72 s, for no heights versus heights, respectively; $p < 0.0001$). To address whether the increased latency was due to an increased attentional demand required to step onto the plank as opposed to a wider floor, we quantified the percentage of time subjects spent looking at or around the plank (within 10 cm) as a function of the total time spent visually scanning. Subjects spent the majority of their time looking away from the plank in the heights condition (82% + 2.8%), suggesting that the delay in stepping onto the plank is not due to motor planning. The percentage of time spent looking away from the plank region was not significantly different in subjects who experienced the "no heights" condition (Figure 2K). Similar to the results on visual scanning, latency to step onto the plank positively correlated with the magnitude of change of SCL after heights exposure (Figure 1M). Individuals who had a larger SCL increase had a longer suppression of action ($rho_{spearman} = 0.73$, $p < 0.0001$). Since change in SCL correlated with both visual scanning and suppression of action, and these two variables correlated with each other (Figure S1A), we asked how much SCL and scanning contribute to the delayed latency to step onto the plank. We fit a linear model to explain latency response with a combination of SCL and total scanning distance. This approach revealed a significant contribution of both variables ($p = 0.011$ for SCL and $p < 0.0001$ for scanning; Figure S1B for model details), suggesting that physiological arousal and the amount of visual scanning both contribute significantly to the suppression of action induced by heights.

Subjects with High Anxiety Show Increased Visual Scanning

Physiological hyperarousal is common to anxiety disorders.[9] It is not known, however, how physiological hyperarousal and trait anxiety impact threat responses. We explored this by measuring physiological arousal, visual scanning, and inhibition of approach in response to heights in subjects with high generalized anxiety or high trait anxiety, but who did not report phobic levels of fear of heights. We recruited subjects who scored higher than 10 on the GAD-7 anxiety questionnaire and had a trait anxiety score > 45 on the State Trait

Anxiety Inventory (STAI; Tables S1 and S3 for subject information).[32] We tested if they had higher levels of spontaneous physiological arousal by measuring the number of spontaneous SCRs they experienced while performing the cognitive task before the sight of heights. Anxious subjects had a significantly higher number of SCRs before the sight of heights, indicating baseline hyperarousal (Figures 3A–3C; mean ± SEM = 1.51 ± 0.19 and 2.18 ± 0.23, for control and anxious subjects, respectively; $p = 0.028$). There was also a trend toward hyperarousal in response to heights as quantified by the increase in amplitude and duration of the SCR. However, this was not significant due to high variability (Figures 3A, 3B, 3D, and 3E; SCL change, mean [Z score] ± SEM = 7.45 ± 1.26 and 12.86 ± 5.58, for control and anxious, respectively; $p = 0.24$; SCR duration, mean ± SEM = 20.78 ± 2.45 s and 31.07 ± 7.24 s, for control and anxious, respectively; $p = 0.11$). In summary, anxious subjects exhibited greater levels of physiological reactivity before exposure to visual threat and a trend toward a longer and higher amplitude SCR to visual threat exposure.

Next, we tested if anxious subjects had altered visual scanning behavior to heights. They exhibited increased scanning quantified by (1) significantly longer total scanning distance and (2) a significantly greater number of visual scans to heights as compared to non-anxious control subjects (Figure 3H; mean ± SEM = 7.46 ± 1.09 m and 13.85 ± 2.51 m, for control and anxious, respectively; $p = 0.002$; Figure 3I; mean number of visual scans ± SEM = 2.65 ± 0.32 and 5.37 ± 0.75, for control and anxious, respectively; $p = 0.0018$; Video S2). Visual scanning of anxious subjects did not, however, differ from that of non-anxious subjects in the “no heights” condition or during the VR introduction period, as compared to non-anxious controls (Figures 3H–3J; STAR Methods; total scan distance, mean [no heights] ± SEM = 3.64 ± 0.84 m and 3.66 ± 0.49 m, $p = 0.99$; mean [VR intro] ± SEM = 6.15 ± 0.82 m and 5.07 ± 0.72 m, $p = 0.33$; number of scans, mean [no heights] ± SEM = 1.53 ± 0.78 and 1.76 ± 0.21, $p = 0.57$; mean [VR intro] ± SEM = 2.13 ± 0.32 and 1.64 ± 0.23, $p = 0.21$; average scan distance, mean [no heights] ± SEM = 1.65 ± 0.19 m and 1.18 ± 0.13 m, $p = 0.08$; mean [VR intro] ± SEM 1.20 ± 0.15 m and 1.17 ± 0.12 m, $p = 0.85$, for control and anxious, respectively). Interestingly, the average distance covered by individual visual scans was shorter in anxious subjects than in healthy controls (Figure 3J; mean ± SEM = 1.57 ± 0.14 m and 1.31 + 0.67 m, $p = 0.04$). Similar to the control subjects, anxious subjects spent the majority of their scanning time away from the plank (Figure 3K; 86% ± 2.7% and 85% ± 1.4%, $p = 0.39$, for control and anxious subjects, respectively). The total scanning distance by each subject correlated significantly with the duration of their SCR to heights (Figure 3L; $rho_{spearman} = 0.76$, $p < 0.0001$), but not their subjective anxiety scores (trait anxiety, $rho_{spearman} = 0.15$, $p = 0.38$; state anxiety, $rho_{spearman} = 0.23$, $p = 0.20$; GAD-7, $rho_{spearman} = 0.16$, $p = 0.38$) or their subjective fear of heights (data not shown). These results indicate that subjects with high trait anxiety are more likely to have hyperarousal to threats, and that correlates with their amount of visual scanning, but not to their subjective fear or anxiety. The results emphasize the importance of quantifying physiological arousal, and not just subjective anxiety, in order to understand human responses to visual threat.

We also tested if anxious subjects exhibited increased inhibition to approach the task. Reduction in approach behavior has been linked to anxiety.[29,30] Anxious subjects’ latency to step onto the plank was significantly greater than the healthy controls (Figure 3M; mean ± SEM = 6.34 ± 0.72 s and 13.1 ± 2.28 s, $p = 0.002$, for control and anxious subjects,

respectively) and latency to first step significantly correlated with the duration of their SCR to heights (Figure 3N; $rho_{spearman} = 0.8$, $p < 0.0001$). The anxious subjects did not subjectively rate the heights experience as significantly scarier or real (Figure 3O; mean fear rating ± SEM = 2.17 [out of 5] ± 0.18 and 2.64 ± 0.20, p = 0.08; mean "real" rating ± SEM = 3.32 [out of 5] ± 0.02 and 3.01 ± 0.03, p = 0.47, for control and anxious subjects, respectively). This suggests that physiological arousal is a better predictor of behavioral responses than is a subjective report of fear, underscoring the value of pairing multiple physiological measures of autonomic tone with subjective reports when studying anxiety and threat. Unlike control subjects, anxious subjects' feelings of "realness" and "scariness" were significantly correlated ($rho_{spearman} = 0.56$, $p < 0.001$), suggesting that anxious subjects were more likely to perceive something as more real if it was also scarier and vice versa. Interestingly, we found that behavioral immobility and visual scanning were both longer in females than in males, although the trend was present in both sexes (Figures 4A and 4B; latency to step, male mean ± SEM = 5.50 ± 0.62 s and 6.91 ± 1.28 s, for control and anxious, respectively; p = 0.27; female mean ± SEM = 6.98 ± 1.18 s and 15.40 ± 2.99 s, for control and anxious, respectively; p = 0.01; total gaze distance, male mean ± SEM = 6.11 ± 0.73 m and 9.05 ± 1.52 m, p = 0.06; female mean ± SEM = 8.67 ± 1.94 m and 15.66 ± 3.36 m, p = 0.11). Although it wasn't the focus of this study, we found that anxious subjects performed significantly worse on the cognitive task than did the healthy controls, a difference that became even more robust after being exposed to heights and crossing the plank (Figure S2; mean [task score] ± SEM = 1.31 ± 0.2 and 0.58 ± 0.15 for control and anxious, respectively; p = 0.01). These findings are consistent with increased executive functioning defects in people with anxiety disorders.[9]

Roles of Human Insula and Orbitofrontal Cortices in Human Visual Threat Processing

A major unresolved issue in the study of human fear and threat responses is the relationship between central nervous system (CNS) signals and peripheral physiology, in particular the temporal relationship. To assess brain regions involved in visually driven arousal, and to relate those to peripheral measures of arousal, we simultaneously recorded intracranial electroencephalography (iEEG) signals, skin conductance, and eye movements from epilepsy patients implanted with intracranial electrodes for seizure localization (Figure 5A; Video S3; STAR Methods; Table S1 for subject information). The locations of the electrodes were constrained by clinical needs (Figures 5A and S3). We selected patients with electrodes in their insula and orbitofrontal cortex (OFC), as these structures are implicated in somatic awareness and emotional regulation (Figures 5A, 5B, and 6A).[33–37] We tested whether insula or OFC activity correlated with SCR in response to heights. We recorded from a total of 3 patients (Figure S3). Two patients who had electrodes in the insula (subjects: EC 192 and EC 205; Figure S3) and two patients who had electrodes in the OFC (EC 200 and EC 205; Figure S3). One patient had electrodes in both the insula and the OFC (EC 205). Insula electrodes were located in the following order: 53 (most posterior), 54, 3, 2, 21, 16 (most anterior). In the OFC, the electrodes were located in the following order: 98 (most posterior), 99, 12, 14, 6, 1, 2 (most anterior; Figures 5A and S3).

The patients viewed a version of the heights stimulus that was modified to fit the mobility constraints of the patients in the hospital room (Figure 5D; STAR Methods; Video S3). We

simultaneously recoded iEEG and skin conductance signals (Video S3). iEEG signals were processed offline to remove 60 Hz line noise and motion artifacts using standard methods (Figure S4; STAR Methods).[38–40] Normalized amplitudes in different frequency bands were calculated (4–8 Hz [theta], 8–15 Hz [alpha], 15–40 Hz [beta], 40–70 Hz [low gamma], 70–150 Hz [high gamma]; STAR Methods). We observed that the fast rises in the high gamma activity in the insula correlated with the fast spikes of the skin conductance level that occurred in response to the appearance of heights (Figure 5E). This was also apparent during the viewing of a 360-degree movie of swimming with sharks, which subjects rated as moderately "scary," compared to heights, which they ranked higher on the "scary" scale (Figures S5A–S5C). SCRs represent the phasic, fast, stimulus-driven component of the SCL. SCL was processed to extract phasic and tonic components to analyze the relationship between both fast and slow components of the skin conductance signal (STAR Methods).

We analyzed the amplitude of the iEEG signal at all frequency bands from 6 insula electrodes from 2 patients (Figure 5B) and observed a significant correlation between high gamma activity in the insula and SCR during the viewing of virtual heights from both patients (Figure 5F; $rho_{spearman} = 0.41$, $p = 0.002$; see Table S4 for correlation coefficients for each patient for each frequency band). There was no correlation between the insula activity and skin conductance during the "no heights" condition when subjects merely viewed the simulated hospital room in VR (Figure 5G; Table S4). This suggests that the insula is specifically involved in visual threat-driven, but not spontaneous, physiological arousal. Cross-correlation analysis of SCR and insula high gamma activity across all electrodes revealed a peak at 8 s, suggesting that insula activity precedes SCR by 8 s (Figures 5H and 5I). To assess the significance of that correlation, we performed a permutation analysis where we sampled the insula activity in 100 ms bins and shuffled it in time 1,000 times. We then calculated the correlation coefficients between insula and SCR (STAR Methods) each time. For 5 out of 6 insula electrodes, the correlation coefficients for real insula time series were significantly higher than the distribution of correlation coefficients produced by the random permutation (Figure 5J; $p < 0.0001$). Interestingly, the correlation was the strongest in the electrodes located most posteriorly (channels 53, 54), and it became weaker toward the anterior insula and was absent in the most anterior electrode (channel 16). It is worth noting that both patients with insula electrodes scored high on the GAD-7 generalized anxiety scale, similar to the anxious subjects in the mobile heights set-up.

We recorded signals from the OFC from 7 electrodes in 2 patients (Figure 6A). We observed a significant negative correlation between OFC low frequency theta activity and SCR during heights exposure (Figure 6B; $rho_{spearman} = -0.44$, $p = 0.001$), but not during the "no heights" condition when the subject was viewing the virtual hospital room (Figure 6C; $p = 0.07$). Cross-correlation from all OFC electrodes revealed 2 troughs: one at −2 s and another at 12 s (Figures 6D and 6E), suggesting that OFC theta was suppressed ~12 s prior to SCR and remained suppressed until after 2 s of SCR. The strongest anti-correlations between theta and SCR were observed in the most posterior region, closest to the insula (98, 99, 12). Permutation analysis revealed that this negative correlation was significant for all except 1 OFC electrode (Figure 6F). This is different from what we observed from our recordings of neural signals from the insula, which showed a positive correlation between theta activity

and SCR (Table S4). Similar to the insula, we found a trend toward a positive correlation between OFC gamma and SCR (Table S4). However, this was significant only in one patient. Overall, our results suggest an increase in insula and OFC gamma activity, and a decrease in OFC theta activity, prior to visually evoked arousal.

We also tested whether insula and OFC activity were related to the anxiety-associated visual scanning behavior described earlier. All patients we recorded neural activity from were able to freely move and rotate their heads and look down at heights, despite the experimental (wire) tethers attached to the VR headset and their implanted electrodes (Figure 7A; Video S3). Patient EC 200 had no visual scanning episodes during heights, which we attributed to her low anxiety score. We extracted visual scanning episodes as described (STAR Methods) and calculated the high-gamma amplitude in the insula amplitude before and during the visual scanning episode (Figures 7B and 7C). We found that the gamma amplitude from 5 out of 6 insula electrodes (4 from EC 192 and 1 from EC 205) was significantly higher during visual scanning compared to the 10 s before scanning, in all 5 scanning episodes (3 from EC 192, 2 from EC 205) (Figure 7C; $p < 0001$). One insula electrode (#16) from patient EC 205 had a decrease in gamma during a visual scanning. Interestingly, this electrode was located in the anterior as opposed to the more posterior insula locations of the other electrodes, and didn't have significant correlation with SCR. Differences between anterior and posterior insula may explain why the activity from this electrode didn't increase during visual scanning.[41–43] We observed that the majority of the visual scanning during the shark stimulus was accompanied by an increase in gamma activity in the insula; however, this was not statistically significant (Figures S5C and S5D; $p = 0.296$). These experiments revealed the presence of higher gamma activity in the insula during arousal-related visual scanning behavior, supporting the view that visual scanning of threat-inducing stimuli and their surrounding environment reflect the activity of defined brain networks involving the insula.

DISCUSSION

Our results suggest that visual scanning is a robust behavioral readout of physiological arousal in response to visual threat in humans. This behavior was significantly lower in an equally ambiguous but less physiologically arousing "no heights" stimulus (i.e., in either scenario subjects were not told in advance what would happen during the task). The amount of scanning correlated with level of sympathetic arousal in both healthy and anxious subjects despite not correlating with subjective measures of anxiety. Previously, a reduction in visual scanning was reported in response to heights in subjects with phobias of heights.[44,45] We only included subjects without fear of heights, and thus, taken with the previous work, ours shows that eye movements can be used to assess acute fear of heights versus generalized anxiety. We found that while having high trait anxiety makes a person more likely to respond with increased visual scanning, the level of physiological arousal to threat is more predictive of the level of scanning a subject will exhibit than is the person's own subjective measures of reported anxiety. This matches a previous study linking head movements to subjective reports of arousal in virtual environments.[46,47] Collectively, our results indicate that increases in visual scanning behavior are a universal readout of heighted arousal and

anxiety.[27,28,46–48] In future studies, we hope to test for a causal role of eye movements in fear and anxiety states.

In addition to shifts in visual scanning, subjects with more physiological arousal also had longer latencies to step out onto the bridge. Suppression of active or appetitive behaviors in responses to a Pavlovian threat has been previously used as a model for response impairment in anxiety disorders.[29–31] Our results reveal that suppression of active behavior occurs also to non-conditioned, non-Pavlovian threats such as heights, in both healthy and anxious subjects.

We consistently observed increases in physiological arousal that preceded the onset of visual scanning behavior (Videos S1 and S2). We acknowledge that scanning behavior exposes subjects to the heights for a longer time, triggering more arousal. Anxious subjects tended to get stuck in a feedback loop between a heightened arousal state and visual scanning, and thus more exposure to heights, which prevented them from stepping onto the bridge (Video S2). This suggests interventions that shift visual focus away from impending threats or that intervene with scanning behavior may prove effective in decreasing physiological arousal and/or reduce the delay for goal-directed approach.

Our real-time recordings from the human brain revealed that high-frequency gamma activity in the insula correlates with phasic skin conductance and visual scanning behavior during viewing of visual threats (Figure 5). The insula has been implicated in bodily self-awareness, emotion regulation,[49,50] social anxiety,[51,52] and consciousness.[53] The correlation between insula activation and phasic skin conductance is generally consistent with findings that the posterior insula acts as a readout of physiological arousal.[34,42] Here, the insula's link to arousal only occurred during direct exposure to visual threat. We also show that insula is activated during visual scanning of threats. Recent work from Gehrlach et al.[34] in rodents showed a role for insula for processing bodily states and shifting behavioral strategies. Our results suggest that the insula may play a similar role in humans by integrating physiological arousal and visual scanning behavior. The insula has been shown to be a central station in the defense network[51] with connectivity to both cortical and subcortical regions.[54] fMRI studies have shown co-hyper-activation of insula and amygdala during high fear and anxiety.[1,34,51] We plan to investigate the role of amygdala in visually induced arousal in future studies by recording from more subjects, including those with electrodes in amgydalar subregions.

Here we also show a suppression of OFC low-frequency theta activity during SCRs (Figure 6). This is consistent with work describing that OFC is implicated in interpretation of somatic states and mood disorders as well as reward value estimation and decision making.[37] Our results support OFC's role in emotional and somatic states and extend those to specific modes of anxiety-related visual threat processing. Other regions in the defensive network such as ventral hippocampus and anterior cingulate cortex have been implicated in regulatory roles during threat processing and mood disorders.[38–40] Simultaneous recordings from these regions with the insula and OFC in the future studies will illuminate their role in the dynamics of the defensive network and induced behavior during visually induced realistic threats. The fact that visual scanning is a direct, non-invasive readout of CNS

activity such as the insula that detect saliency and threat, and the reciprocal relationship between anxiety and visual scanning, suggests that eye movements are a tractable feature for monitoring and adjustment of arousal in humans. We plan to investigate the causal relationship between eye movements and arousal by transient silencing or activation of brain areas such as the insula as well as controlling eye movements directly using VR.

Limitations and Considerations

The data here support the idea that eye movements, as well as activation dynamics in the insula and OFC, may play important roles in the process by which humans detect and respond to visually evoked threats. These variables may therefore be informative toward building objective measures of anxiety and for developing treatment interventions for anxiety-related conditions. We wish to emphasize that the intracranial recordings in this study were obtained from a limited number of human subjects (n = 3). These subject numbers are not atypical for non-case-study experiments with human intracranial recordings (Miller et al., n = 1;[55] Aghajan et al., n = 3;[20] Mesgarani and Chang, n = 3[56]). Nonetheless, we acknowledge the limitations to the interpretive power of studies performed on a limited number of individuals and therefore can only preliminarily conclude about the causal involvement of insula gamma and OFC theta activity for visual threat responses at this time.

STAR★METHODS

RESOURCE AVAILABILITY

Lead Contact—Further information and requests for resources and reagents should be directed to and will be fulfilled by the Lead Contact, Andrew Huberman (adh1@stanford.edu).

Materials Availability—This study did not generate new unique reagents.

Data and Code Availability—The original datasets and code generated during this study have been deposited to Dryad repository: https://doi.org/10.5061/dryad.wdbrv15mq

EXPERIMENTAL MODEL AND SUBJECT DETAILS

All experiments at Stanford were conducted under the approved IRB #41398 with written informed consent. Subjects over 18 years of age were recruited through fliers and online advertisement on and off campus. They were prescreened for reported mental illness or neurological condition. Subjects with no reported history of mental illness or neurological condition and also scored lower than 10 in the GAD-7 and 45 in both State and Trait subscales of the STAI were invited to the study as “healthy subjects.” Subjects who scored higher than 9 on GAD-7 and/or higher than 45 in STAI Trait Anxiety were recruited as “anxious.” See Table S1 for subject information for each group of subjects. Many of the qualified anxious subjects also reported comorbid depression and/or other mental disorders. Applicants were excluded if judged too severe by their survey responses by Stanford Psychiatrist Dr. Bhati or answered “yes” to “Have you considered suicide within the last month”? question. Reported comorbidity and medication status are reported in Table S3. All

subjects were also screened for a heights phobia using self-report and DSM-V criteria. No subject with a heights phobia were run on the heights stimulus.

iEEG Recordings took place at the UCSF Hospital on epilepsy patients under Dr. Eddie Chang's care as described in Rao et al.[59] Briefly, iEEG electrodes were surgically implanted in subjects with treatment-resistant epilepsy for localization of seizure foci. All subjects provided written consent to participate in this study. The procedures were approved by the University of California, San Francisco Institutional Review Board (See Table S1 for subject age and sex information). Subjects were included in the study if they had electrodes in the regions of interest and willing to participate in the VR task. Electrode implantation was guided solely by clinical decision for optimal seizure monitoring.

METHOD DETAILS

Virtual Reality—Heights and 'No heights' stimuli were custom programmed using the Unity game engine. HTC Vive headset with embedded Tobii eye-tracker were used for presentation of the VR stimuli. All experiments except with intracranial recordings took place at the newly built Huberman VR Lab (Figure 1A), which is an 8×13 ft space with a 5×11 ft observation area with padded floors and walls and an in-house built cable management system to avoid having the experimenter carry the headset cable during the experiment.

Virtual Reality Stimuli—Subjects were randomly assigned to a heights or 'no heights' stimulus. All subjects were instructed to a cognitive task called 'Lights out' in the VR room modeled to look like the actual experiment room. The task had two purposes: 1. provide the interactivity subjects needed to feel immersed in the virtual environment 2. give the subjects a goal to approach to measure inhibition of goal directed approach in response to heights. It consists of a 4 by 4 light grid. A random selection of lights is "ON" at the start. Clicking on a light toggles it and the lights adjacent to it. The goal is to turn off all the lights by clicking on them. Subjects score points by turning off all the lights on the grid, after which the grid re-sets with a different light combination.

The task was presented on the right wall of the room and subjects played with their backs turned to the rest of the room. While they were engaged in the task, the walls, middle of the floor (except for the plank) and the ceiling fell away. One minute into the task during the heights stimulus, the task board moved to the other side of the room. The subjects had to step on a high and narrow plank to continue playing and scoring points. The task was visible on the other side of the plank and was marked with arrows pointing to the floor that says, "Step here to play." During the "No heights" stimulus the room walls and ceiling opened up similar to the heights, but floor didn't drop. Thus, there was no sensation of heights. The subjects still experienced a change in visual environment, and they needed to walk across to the other side in order to continue the task. At the 3-min mark the task moved back to its original location and subjects needed to walk back across one more time to continue. In the current paper, we only report the results from the first cross to avoid the confound of habituation at the second cross. At the end of the 4 min, subjects were asked to fill out a

survey ranking how “scary” and “real” they found the task on a scale of 1 to 5, 1 being “not at all” and 5 being “extremely.”

All subjects were explained that they could take out the headset, take a break or leave the experiment if they felt uncomfortable. 2 anxious subjects opted to stop the experiment after the introduction period before seeing the actual stimulus. None of the healthy controls opted out of the experiment.

Modified Heights Stimulus—Heights stimulus was modified to fit the mobility constraints of the epilepsy patients at UCSF Medical center. In this version of the stimulus, subjects were sitting in a chair and the virtual room was modeled as the hospital room they were in. They played the ‘lights-out’ task situated in front of them. 1 min into the task the walls and the floor of the virtual room start falling down such that the subject is left sitting in a chair on a platform of a building 50 stories high. Subjects typically showed visual scanning of their environment during this period while continuing the task, similar to the original heights experience (Video S3). Before the heights stimulus each subject’s baseline brain activity and skin conductance were measured for five minutes while they were exposed to the virtual hospital room but were not exposed to heights stimulus (‘No Heights’ condition in Figures 5, 6, and S4 and Table S4).

Physiology and Gaze Measurement—Skin conductance, electrocardiogram and respiration were recorded using the BIOPAC MP150 data acquisition system in combination with the wireless BioNomadix system. All subsequent analysis was done in MATLAB with custom code. Gaze data was recorded using the Tobii Pro eye tracker embedded in the HTC Vive Virtual Reality headset for majority of the subjects. The first 4 subjects’ gaze data was recorded using SMI eye tracker integrated into the HTC Vive headset. The SMI eye tracker was discontinued during the study so we switched to Tobii. SMI and Tobii’s SDKs were used to integrate with Unity. Gaze data was analyzed subsequently in MATLAB.

Data Inclusion Criteria and Quality Control (Physiology and Gaze Data)—When subjects were freely moving data quality was sometimes compromised due to subjects touching sensors or electrode contacts moving. To include the maximum amount of data, we grouped data by type (respiration, SCL, etc.) and poor-quality data was excluded. Specifically, subjects with drops in SCL signal due to poor contact or physically touching the electrodes were eliminated (12/52 control subjects (heights), 10/42 control subjects (no heights), 13/37 anxious subjects (heights)). Subjects with motion artifacts in raw ECG were eliminated from heart rate analysis (17/52 control subjects (heights), 3/42 control subjects (no heights)). Subjects without regular breathing pattern (inspected visually during 1 min before or after sight of heights) were eliminated from respiration analysis as this meant the respiration belt lost contact (18 / 52 healthy subjects (heights), 15/42 healthy subjects (no heights)).

For gaze analysis, we had a temporary difficulty with the embedded eye-tracker system and had to replace it; thus no gaze data were collected from 12 subjects during this time. Gaze data from all other subjects were included. Epilepsy subjects sometimes moved their heads

due to discomfort during VR. “False visual scans” from these movements were extracted from the visual scan analysis.

Behavioral Recording—Subject behavior was recorded on a webcam installed to the ceiling of the VR room throughout the experiment. The webcam video was synchronized with the physiology data using the “Media” feature of Acqknowledge software by BIOPAC. A screenshot view of the Acqknowledge window was recorded throughout the experiment for each subject. These videos were manually annotated to extract time stamps for first sight of heights and first step onto the plank which were used to calculate latency to step onto the plank.

Intracranial Electroencephalography (iEEG) Recordings and Electrode Localization—The VR headset secured to each patient’s head using a custom Velcro cap. Electrophysiological recording were acquired at a sampling rate of 3051.8 Hz using a 256-channel PZ2 amplifier or 512-channel PZ5 amplifier connected to an RZ2 digital acquisition system (Tucker-Davis Technologies, Alachua, FL, USA). iEEG signals were recorded for 5 min prior to the onset of the modified heights stimulus for the “No Visual Stim” condition and during the modified heights stimulus. Subjects underwent pre-operative 3 Tesla brain magnetic resonance imaging (MRI) and post-operative computed tomography (CT) scan to localize electrodes. Electrode locations were visualized by co-registering pre-operative T1-weighted MRI with the post-operative CT using Statistical Parametric Mapping software SPM12[59,60] and confirmed by neurologist. Pial surface 3D reconstructions were created using FreeSurfer.

QUANTIFICATION AND STATISTICAL ANALYSIS

Physiology and Gaze Analysis—All data are analyzed in MATLAB using custom scripts (available at Dryad repository: https://doi.org/10.5061/dryad.wdbrv15mq). Physiology data, collected by Biopac wireless BioNomadix system, was down sampled to 200 Hz. Signals 45 s before and after sight of heights were extracted and z-scored relative to the total 90 s period. Visual search distance was defined as the total Euclidian distance between points of gaze when subjects see heights before stepping onto the plank. Gaze velocity was calculated from the gaze position data and visual scanning was defined as episodes where velocity exceeded 0.2 m/s for more than 0.5 s. % time spent looking at the plank was calculated by dividing total time where gaze was on or within 10 cm of the plank during the heights and the coordinates of the plank + 10 cm during the no heights condition. % time looking away from the plank was 1 minus this number. For correlation analysis with brain activity, tonic and phasic components of the SCL signal was extracted using the cvxEDA free algorithm (https://github.com/lciti/cvxEDA). Sample sizes, descriptive statistics (mean, median, SEM), statistical tests and associated p – values are shown in Table S2.

iEEG Preprocessing—Raw iEEG signals were preprocessed offline (MATLAB) to remove non-neural activity using standard steps as previously reported.[59,60] Briefly, the recordings were down-sampled to 400-Hz sampling rate and notch filtered to eliminate line noise frequency of 60 Hz and harmonics (60, 120, 180 Hz). Common average referencing

(CAR) was performed across all channels sharing the same lead (Figures S4A and S4B). In calculating the reference, channels and time epochs that had been marked as noisy, determined by visual inspection for large amplitude activity, were excluded to prevent noise from spreading to other channels through the CAR. Only electrode contacts located in the target region of interest (verified by visual review of MRI and CT) were analyzed.[59] Data quality for each channel were verified with a power analysis. Channels whose periodograms showed a 1/f distribution over power were considered “good” channels and were included in the analysis. Channels for extra peaks in the high frequency domains in the periodogram were considered “bad” channels and were excluded from the analysis (Figures S4C and S4D). For each subject, the raw iEEG signals were visually inspected for large amplitude seizure activity and non-physiological synchronized activity across channels. Channels with this activity were eliminated from the analysis. Examples of raw data for included and excluded channels shown in Figure S4.

Accordingly, 1 electrode out of 5 in the insula was not analyzed due to noise for EC 192 (channel 43, Figure S4D). For EC 200 1 out of 3 OFC electrodes was not analyzed. Data quality was good for all EC205 electrodes in the insula and OFC and no electrode was excluded from analysis.

Neural Spectral Feature Extraction—Power features from four frequency bands: 4 – 8 Hz (theta), 8–15 Hz (alpha), 15–40 Hz (beta), 40 – 70 (low gamma), 70–150 Hz (high gamma) extracted by filtering the iEEG signal within these bands (Hilbert Transform). Data were smoothed by averaging over 5 s windows (no overlap). Smoothed data was z-scored in MATLAB relative to length of the recording (~300 s). Spearman correlation was used to calculate the relationship between z-scored power of iEEG spectral bands and z-score of phasic skin conductance signal.

Supplementary Material

Refer to Web version on PubMed Central for supplementary material.

ACKNOWLEDGMENTS

We thank Troy Allen Norcross and Game Hearts Co. for their help in programming the VR stimuli; Adam Osfield Snell, Vrtul team, and Dogz101 RWC for helping shoot and produce 360 movies; Dr. Mahendra Bhati for his help in qualifying anxious subjects for our study; Dr. Mauricio Hoyos and the Semarnat Authority (Secretaría del Medio Ambiente y Recursos Naturales) for permission to film the 360 movies of great white sharks at the Guadalupe Is. Field Station; Michael Muller and team for VR movie filming of sharks; members of the Chang Lab for helping with logistics to record from epilepsy patients; Gary Holl for ongoing infrastructure operations of the Huberman VR Laboratory; and Heekyung Jung, and Supraja Varadarajan for comments on the manuscript. This work was supported by a Discovery Innovation Award from Stanford School of Medicine (A.D.H.), Stanford School of Medicine Dean’s Fellowship (M.Y.B.), the Shurl and Kay Curci Foundation (E.F.C.), the William K. Bowes Foundation (E.F.C.), and R01-DC012379 (E.F.C.).

REFERENCES

1. Craske MG, Stein MB, Eley TC, Milad MR, Holmes A, Rapee RM, and Wittchen HU (2017). Anxiety disorders. Nat. Rev. Dis. Primers 3, 17024. [PubMed: 28470168]
2. Buff C, Brinkmann L, Neumeister P, Feldker K, Heitmann C, Gathmann B, Andor T, and Straube T (2016). Specifically altered brain responses to threat in generalized anxiety disorder relative to social anxiety disorder and panic disorder. Neuroimage Clin. 12, 698–706. [PubMed: 27761400]

3. Feldker K, Heitmann CY, Neumeister P, Tupak SV, Schrammen E, Moeck R, Zwitserlood P, Bruchmann M, and Straube T (2017). Transdiagnostic brain responses to disorder-related threat across four psychiatric disorders. Psychol. Med 47, 730–743. [PubMed: 27869064]
4. Yilmaz M, and Meister M (2013). Rapid innate defensive responses of mice to looming visual stimuli. Curr. Biol 23, 2011–2015. [PubMed: 24120636]
5. Salay LD, Ishiko N, and Huberman AD (2018). A midline thalamic circuit determines reactions to visual threat. Nature 557, 183–189. [PubMed: 29720647]
6. Li L, Feng X, Zhou Z, Zhang H, Shi Q, Lei Z, Shen P, Yang Q, Zhao B, Chen S, et al. (2018). Stress accelerates defensive responses to looming in mice and involves a locus coeruleus-superior colliculus projection. Curr. Biol 28, 859–871.e5. [PubMed: 29502952]
7. Weston CS (2014). Posttraumatic stress disorder: a theoretical model of the hyperarousal subtype. Front. Psychiatry 5, 37. [PubMed: 24772094]
8. Kalmbach DA, Cuamatzi-Castelan AS, Tonnu CV, Tran KM, Anderson JR, Roth T, and Drake CL (2018). Hyperarousal and sleep reactivity in insomnia: current insights. Nat. Sci. Sleep 10, 193–201. [PubMed: 30046255]
9. Grisanzio KA, Goldstein-Piekarski AN, Wang MY, Rashed Ahmed AP, Samara Z, and Williams LM (2018). Transdiagnostic symptom clusters and associations with brain, behavior, and daily function in mood, anxiety, and trauma disorders. JAMA Psychiatry 75, 201–209. [PubMed: 29197929]
10. De Franceschi G, Vivattanasarn T, Saleem AB, and Solomon SG (2016). Vision guides selection of freeze or flight defense strategies in mice. Curr. Biol 26, 2150–2154. [PubMed: 27498569]
11. Kim JJ, and Jung MW (2018). Fear paradigms: the times they are a-changin'. Curr. Opin. Behav. Sci 24, 38–43. [PubMed: 30140717]
12. Qi S, Hassabis D, Sun J, Guo F, Daw N, and Mobbs D (2018). How cognitive and reactive fear circuits optimize escape decisions in humans. Proc. Natl. Acad. Sci. USA 115, 3186–3191. [PubMed: 29507207]
13. Mobbs D, Petrovic P, Marchant JL, Hassabis D, Weiskopf N, Seymour B, Dolan RJ, and Frith CD (2007). When fear is near: threat imminence elicits prefrontal-periaqueductal gray shifts in humans. Science 317, 1079–1083. [PubMed: 17717184]
14. Adolphs R (2008). Fear, faces, and the human amygdala. Curr. Opin. Neurobiol 18, 166–172. [PubMed: 18655833]
15. Öhman A, Carlsson K, Lundqvist D, and Ingvar M (2007). On the unconscious subcortical origin of human fear. Physiol. Behav 92, 180–185. [PubMed: 17599366]
16. Blanchard DC, Hynd AL, Minke KA, Minemoto T, and Blanchard RJ (2001). Human defensive behaviors to threat scenarios show parallels to fear- and anxiety-related defense patterns of non-human mammals. Neurosci. Biobehav. Rev 25, 761–770. [PubMed: 11801300]
17. Harrison LA, Ahn C, and Adolphs R (2015). Exploring the structure of human defensive responses from judgments of threat scenarios. PLoS ONE 10, e0133682. [PubMed: 26296201]
18. Bach DR, Guitart-Masip M, Packard PA, Miró J, Falip M, Fuentemilla L, and Dolan RJ (2014). Human hippocampus arbitrates approach-avoidance conflict. Curr. Biol 24, 541–547. [PubMed: 24560572]
19. Camerer C, and Mobbs D (2017). Differences in behavior and brain activity during hypothetical and real choices. Trends Cogn. Sci 21, 46–56. [PubMed: 27979604]
20. M Aghajan Z, Schuette P, Fields TA, Tran ME, Siddiqui SM, Hasulak NR, Tcheng TK, Eliashiv D, Mankin EA, Stern J, et al. (2017). Theta oscillations in the human medial temporal lobe during real-world ambulatory movement. Curr. Biol 27, 3743–3751.e3. [PubMed: 29199073]
21. Reggente N, Essoe JK-Y, Aghajan ZM, Tavakoli AV, McGuire JF, Suthana NA, and Rissman J (2018). Enhancing the ecological validity of fMRI memory research using virtual reality. Front. Neurosci 12, 408. [PubMed: 29962932]
22. Blascovich J, Loomis J, Beall AC, Swinth KR, Hoyt CL, and Bailenson JN (2002). Immersive virtual environment technology as a methodological tool for social psychology. Psychol. Inq 13, 103–124.
23. Cummings JJ, and Bailenson JN (2016). How immersive is enough? A meta-analysis of the effect of immersive technology on user presence. Media Psychol 19, 272–309.

24. Rizzo A, and Shilling R (2017). Clinical virtual reality tools to advance the prevention, assessment, and treatment of PTSD. Eur. J. Psychotraumatol 8 (sup5), 1414560. [PubMed: 29372007]
25. Gonçalves R, Pedrozo AL, Coutinho ESF, Figueira I, and Ventura P (2012). Efficacy of virtual reality exposure therapy in the treatment of PTSD: a systematic review. PLoS ONE 7, e48469. [PubMed: 23300515]
26. Carl E, Stein AT, Levihn-Coon A, Pogue JR, Rothbaum B, Emmelkamp P, Asmundson GJG, Carlbring P, and Powers MB (2019). Virtual reality exposure therapy for anxiety and related disorders: a meta-analysis of randomized controlled trials. J. Anxiety Disord 61, 27–36. [PubMed: 30287083]
27. Blanchard DC, Blanchard RJ, and Rodgers RJ (1991). Risk assessment and animal models of anxiety. In Animal Models in Psychopharmacology, Olivier B, Mos J, and Slangen L, eds. (Springer), pp. 117–134.
28. Blanchard DC, Griebel G, Pobbe R, and Blanchard RJ (2011). Risk assessment as an evolved threat detection and analysis process. Neurosci. Biobehav. Rev 35, 991–998. [PubMed: 21056591]
29. Estes WK, and Skinner BF (1941). Some quantitative properties of anxiety. J. Exp. Psychol 29, 390.
30. Allcoat D, Greville WJ, Newton PM, and Dymond S (2015). Frozen with fear: conditioned suppression in a virtual reality model of human anxiety. Behav. Processes 118, 98–101. [PubMed: 26115568]
31. Greville WJ, Newton PM, Roche B, and Dymond S (2013). Conditioned suppression in a virtual environment. Comput. Human Behav 29, 552–558.
32. Yu Q, Zhuang Q, Wang B, Liu X, Zhao G, and Zhang M (2018). The effect of anxiety on emotional recognition: evidence from an ERP study. Sci. Rep 8, 16146. [PubMed: 30385790]
33. Critchley HD, Wiens S, Rotshtein P, Ohman A, and Dolan RJ (2004). Neural systems supporting interoceptive awareness. Nat. Neurosci 7, 189–195. [PubMed: 14730305]
34. Gehrlach DA, Dolensek N, Klein AS, Roy Chowdhury R, Matthys A, Junghänel M, Gaitanos TN, Podgornik A, Black TD, Reddy Vaka N, et al. (2019). Aversive state processing in the posterior insular cortex. Nat. Neurosci 22, 1424–1437. [PubMed: 31455886]
35. Bechara A, Damasio H, and Damasio AR (2000). Emotion, decision making and the orbitofrontal cortex. Cereb. Cortex 10, 295–307. [PubMed: 10731224]
36. Stalnaker TA, Cooch NK, and Schoenbaum G (2015). What the orbitofrontal cortex does not do. Nat. Neurosci 18, 620–627. [PubMed: 25919962]
37. Rudebeck PH, and Rich EL (2018). Orbitofrontal cortex. Curr. Biol 28, R1083–R1088. [PubMed: 30253144]
38. Allman JM, Hakeem A, Erwin JM, Nimchinsky E, and Hof P (2001). The anterior cingulate cortex. The evolution of an interface between emotion and cognition. Ann. N Y Acad. Sci 935, 107–117. [PubMed: 11411161]
39. Adhikari A, Topiwala MA, and Gordon JA (2010). Synchronized activity between the ventral hippocampus and the medial prefrontal cortex during anxiety. Neuron 65, 257–269. [PubMed: 20152131]
40. Kirkby LA, Luongo FJ, Lee MB, Nahum M, Van Vleet TM, Rao VR, Dawes HE, Chang EF, and Sohal VS (2018). An amygdala-hippocampus subnetwork that encodes variation in human mood. Cell 175, 1688–1700.e14. [PubMed: 30415834]
41. Uddin LQ, Nomi JS, Hébert-Seropian B, Ghaziri J, and Boucher O (2017). Structure and function of the human insula. J. Clin. Neurophysiol 34, 300–306. [PubMed: 28644199]
42. Namkung H, Kim S-H, and Sawa A (2017). The insula: an underestimated brain area in clinical neuroscience, psychiatry, and neurology. Trends Neurosci. 40, 200–207. [PubMed: 28314446]
43. Zhang Y, Zhou W, Wang S, Zhou Q, Wang H, Zhang B, Huang J, Hong B, and Wang X (2019). The roles of subdivisions of human insula in emotion perception and auditory processing. Cereb. Cortex 29, 517–528. [PubMed: 29342237]
44. Kugler G, Huppert D, Eckl M, Schneider E, and Brandt T (2014). Visual exploration during locomotion limited by fear of heights. PLoS ONE 9, e105906. [PubMed: 25165822]
45. Kugler G, Huppert D, Schneider E, and Brandt T (2014). Fear of heights freezes gaze to the horizon. J. Vestib. Res 24, 433–441. [PubMed: 25564086]

46. Won AS, Perone B, Friend M, and Bailenson JN (2016). Identifying anxiety through tracked head movements in a virtual classroom. Cyberpsychol. Behav. Soc. Netw 19, 380–387. [PubMed: 27327065]
47. Li BJ, Bailenson JN, Pines A, Greenleaf WJ, and Williams LM (2017). A public database of immersive VR videos with corresponding ratings of arousal, valence, and correlations between head movements and self report measures. Front. Psychol 8, 2116. [PubMed: 29259571]
48. Blanchard RJ, and Blanchard DC (1989). Attack and defense in rodents as ethoexperimental models for the study of emotion. Prog. Neuropsychopharmacol. Biol. Psychiatry 13 (Suppl), S3–S14. [PubMed: 2694228]
49. Koban L, and Pourtois G (2014). Brain systems underlying the affective and social monitoring of actions: an integrative review. Neurosci. Biobehav. Rev 46, 71–84. [PubMed: 24681006]
50. Phan KL, Wager T, Taylor SF, and Liberzon I (2002). Functional neuroanatomy of emotion: a meta-analysis of emotion activation studies in PET and fMRI. Neuroimage 16, 331–348. [PubMed: 12030820]
51. Etkin A, and Wager TD (2007). Functional neuroimaging of anxiety: a meta-analysis of emotional processing in PTSD, social anxiety disorder, and specific phobia. Am. J. Psychiatry 164, 1476–1488. [PubMed: 17898336]
52. Wang W, Zhornitsky S, Li CS-P, Le TM, Joormann J, and Li CR (2019). Social anxiety, posterior insula activation, and autonomic response during self-initiated action in a Cyberball game. J. Affect. Disord 255, 158–167. [PubMed: 31153052]
53. Craig AD, and Craig AD (2009). How do you feel–now? The anterior insula and human awareness. Nat. Rev. Neurosci 10, 59–70. [PubMed: 19096369]
54. Ghaziri J, Tucholka A, Girard G, Boucher O, Houde J-C, Descoteaux M, Obaid S, Gilbert G, Rouleau I, and Nguyen DK (2018). Subcortical structural connectivity of insular subregions. Sci. Rep 8, 8596. [PubMed: 29872212]
55. Wu H, Miller KJ, Blumenfeld Z, Williams NR, Ravikumar VK, Lee KE, Kakusa B, Sacchet MD, Wintermark M, Christoffel DJ, et al. (2018). Closing the loop on impulsivity via nucleus accumbens deltaband activity in mice and man. Proc. Natl. Acad. Sci. USA 115, 192–197. [PubMed: 29255043]
56. Mesgarani N, and Chang EF (2012). Selective cortical representation of attended speaker in multi-talker speech perception. Nature 485, 233–236. [PubMed: 22522927]
57. Fischl B (2012). FreeSurfer. Neuroimage 62, 774–781. [PubMed: 22248573]
58. Greco A, Valenza G, Lanata A, Scilingo EP, and Citi L (2016). cvxEDA: a convex optimization approach to electrodermal activity processing. IEEE Trans. Biomed. Eng 63, 797–804. [PubMed: 26336110]
59. Rao VR, Sellers KK, Wallace DL, Lee MB, Bijanzadeh M, Sani OG, Yang Y, Shanechi MM, Dawes HE, and Chang EF (2018). Direct electrical stimulation of lateral orbitofrontal cortex acutely improves mood in individuals with symptoms of depression. Curr. Biol 28, 3893–3902.e4. [PubMed: 30503621]
60. Ashburner J, and Friston K (1997). Multimodal image coregistration and partitioning–a unified framework. Neuroimage 6, 209–217. [PubMed: 9344825]

Highlights

- Virtual reality heights trigger autonomic arousal and visual scanning in humans
- Subjects with high trait anxiety display increased visual scanning to threats
- Insula high gamma activity positively correlates with threat-triggered arousal
- Orbitofrontal theta activity negatively correlates with threat-triggered arousal

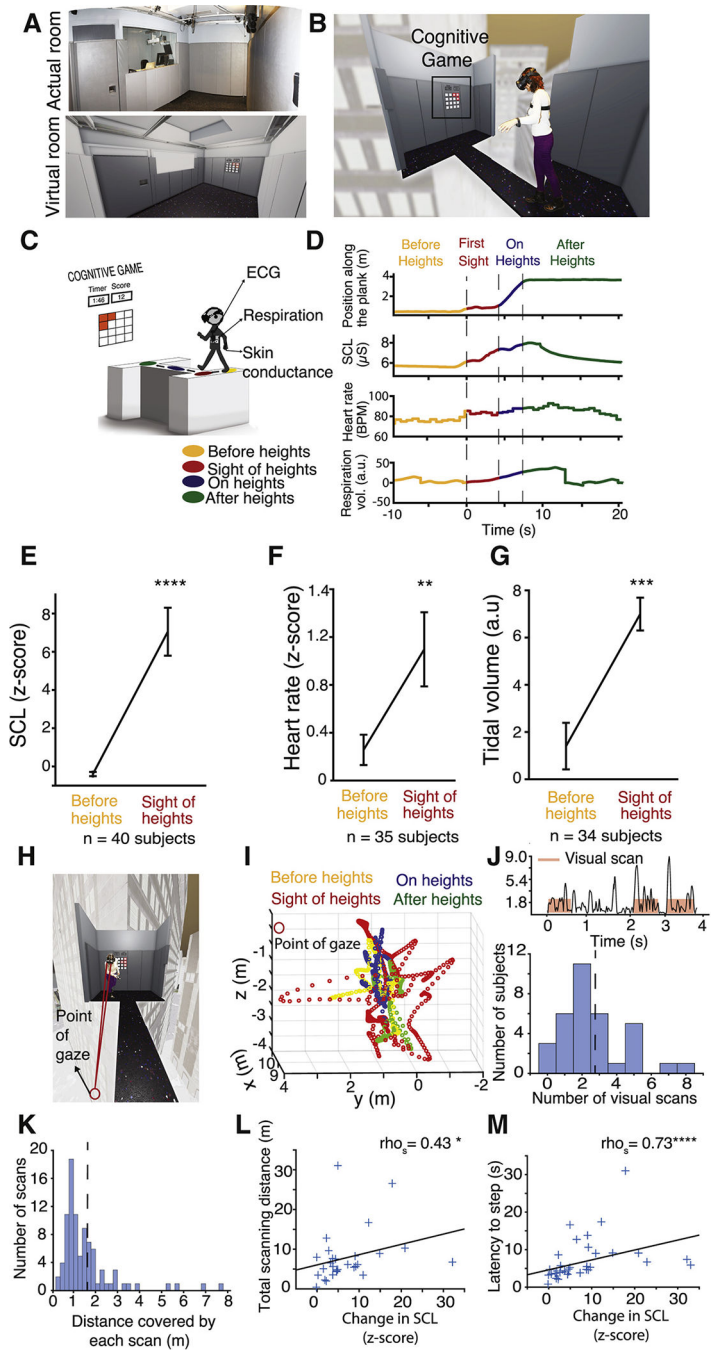

Figure 1. Virtual Heights Reliably Induce Physiological Arousal and Scanning Behavior in Healthy Humans

(A) Views of the real VR room and the virtual room where experiments took place.

(B) Photo of an example subject is superimposed onto the virtual heights stimulus as she is about to step onto the plank.

(C) Schematic of the experience. Skin conductance, respiration, and heart rate are being measured before subject sees heights (yellow), when they see heights before taking a step on the plank (red), while crossing the plank (blue), and after crossing the plank (green).

(D) Example measurements from one subject during the heights experience. The color coding indicates time periods in (C).

(E–G) Skin conductance (E), heart rate (F), and respiration (G) responses before subjects see heights (average of 10 s prior to sight of heights, yellow) and at the time of stepping onto the plank (red) before stepping onto the plank from all subjects. $p < 0.0001$, 0.0077, and 0.001, respectively, based on paired two-sided t test.

(H) Point of gaze in 3D space.

(I) Example gaze location from one subject before (yellow), during (red, blue), and after heights (green). 0,0,0 is the location of the headset.

(J) Example eye velocity trace from one subject after the sight of heights (t = 0). Red rectangles represent automatically calculated visual scan episodes. Below is the histogram distribution of number of visual scan episodes for all healthy subjects in response to heights.

(K) A histogram of all visual scan distances for healthy subjects.

(L) Total gaze distance during heights plotted as function of change in SCL. Spearman correlation coefficient (rho_s) = 0.5, $p = 0.02$.

(M) Latency to step onto the plank as a function of change in SCL. $rho_s = 0.72$, $p < 0.0001$.

See also Figure S1, Table S2, and Video S1.

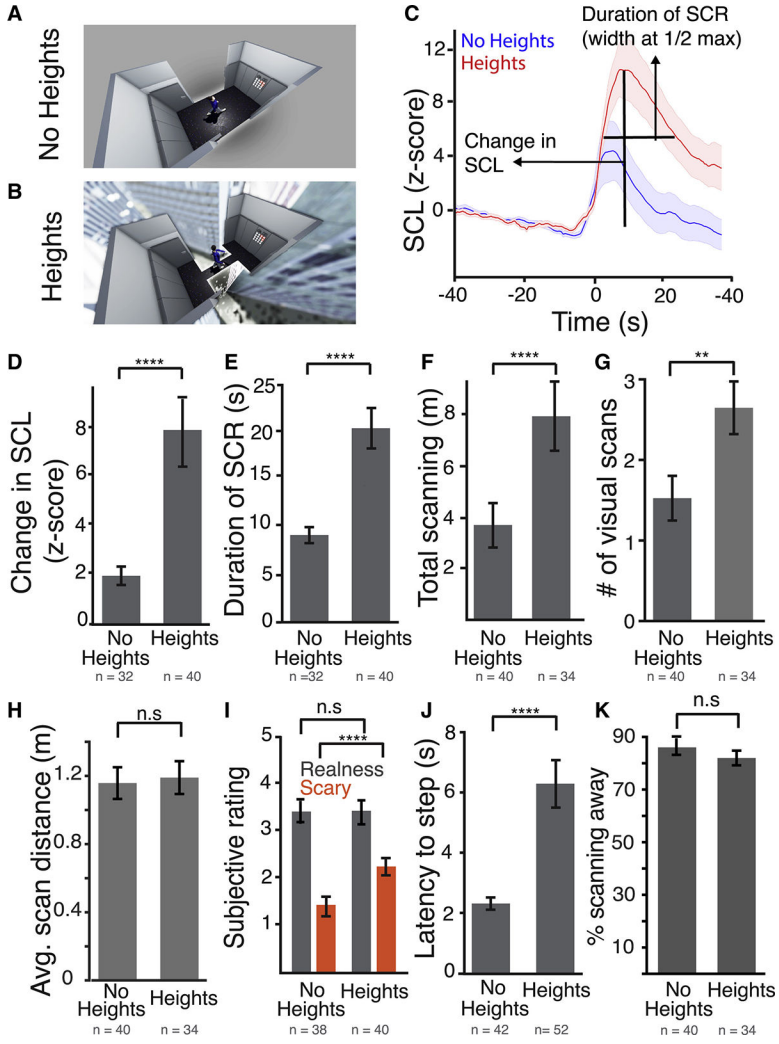

Figure 2. A "No Heights" Control Stimulus Elicits a Lower Level of Arousal, Less Visual Scanning, and Less Inhibition of Goal-Directed Approach

(A) A top camera view of the "no heights" stimulus.

(B) A top camera view of the heights stimulus.

(C) Average waveform of the SCR after sight of the stimulus. Blue, no heights (n = 32 subjects); red, heights (n = 40 subjects).

(D) Average change in SCL in response to both stimuli before crossing to the other side. $p < 0.0001$.

(E) Average duration of the SCR after stimulus presentation for both stimuli. $p < 0.0001$.

(F) Total scanning distance after the sight of both stimuli before crossing. $p < 0.006$.

(G) Average number of visual scans per subject in response to both stimuli. $p < 0.001$.

(H) Average distance covered by each visual scan in response to both stimuli.

(I) Average subjective "realness" and "fear" rating for each stimulus. 1 = did not feel real/scary at all, 5 = felt extremely real/scary. $p < 0.0001$.

(J) Latency to take first step to cross the room in response to both stimuli. $p < 0.0001$.

(K) Percent time spent scanning away from the plank region in response to both stimuli.

Error bars = SEM. p values based on unpaired two-sided t test. n.s., non-significant. See also Table S2.

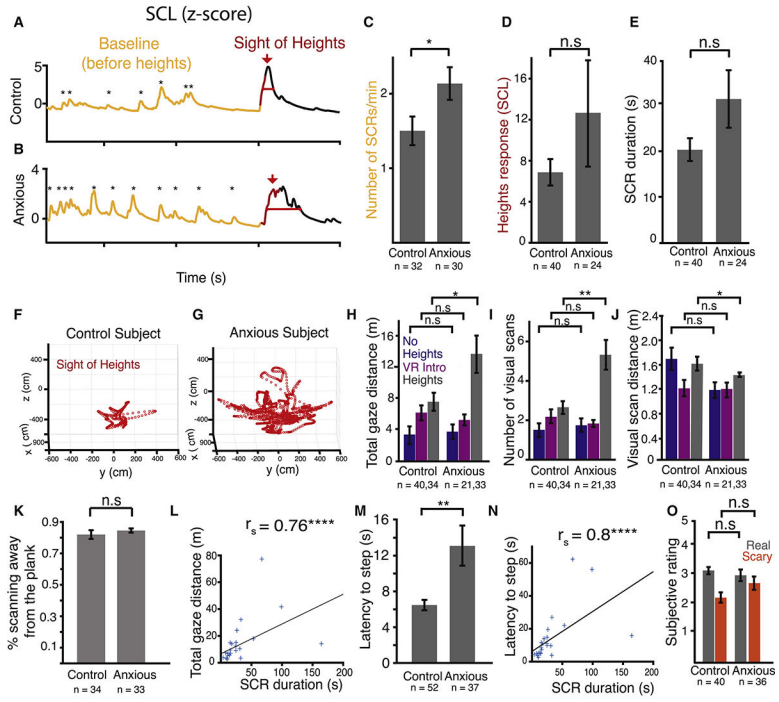

Figure 3. Subjects with High Anxiety Have Increased Visual Scanning and Longer Suppression of Action in Response to Heights

(A and B) Example skin conductance traces from a healthy control (A) and an anxious subject (B) before the sight of heights in VR (yellow) and at the sight of heights (t = 0, red).

(C) Average number of SCRs at baseline for control and anxious subjects. $p < 0.03$.

(D) Average change in SCL after sight of heights before stepping onto the plank.

(E) Duration of the SCR due to heights in control and anxious subjects.

(F and G) Example gaze trajectories from a control (F) and an anxious subject (G).

(H) Average total gaze distance in response to no heights (blue), during VR intro (magenta), and heights (gray) in control and anxious subjects. $p < 0.03$.

(I) Average number of visual scans per subject in response to no heights (blue), during VR intro (magenta), and heights (gray). $p < 0.006$.

(J) Average distance covered by each visual scan during no heights (blue), during VR intro (magenta), and heights (gray) in control and anxious subjects. $p < 0.04$.

(K) Percent time spent looking away from the plank for control and anxious subjects.

(L) Total gaze distance plotted against duration of SCR for each anxious subject. $rho_s = 0.76$; $p < 0.0001$.

(M) Latency to step onto the plank in control and anxious subjects. $p < 0.002$.

(N) Latency to step onto the plank plotted against duration of SCR for each subject. $rho_s = 0.75$; $p < 0.0001$.

(O) Average subjective “realness” and “fear” rating for control and anxious subjects during heights. 1 = did not feel real/scary at all, 5 = felt extremely real/scary.

n.s., non-significant. Error bars = SEM. p values based on unpaired two-sided t test. See also Figure S2, Tables S2 and S3 and Video S2.

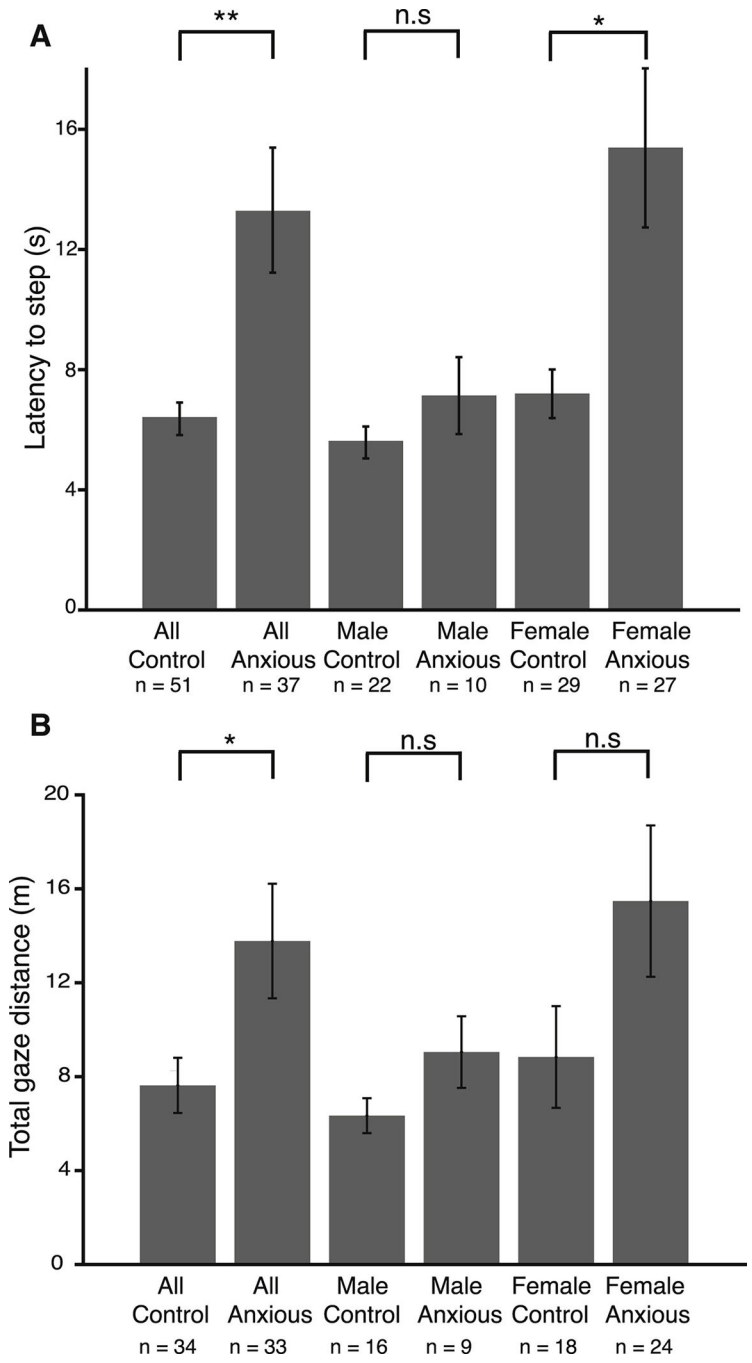

Figure 4. Sex Differences Observed in Anxious Subjects' Heights Responses

(A) Average latency to step onto the plank in all control, all anxious, control male, anxious male, control female, and anxious female subjects. $p < 0.002$ for all subjects, 0.01 for female, 0.27 for males.

(B) Total visual scanning in all control, all anxious, control male, anxious male, control female, and anxious female subjects. $p < 0.03$; n.s., non-significant.

See also Table S2.

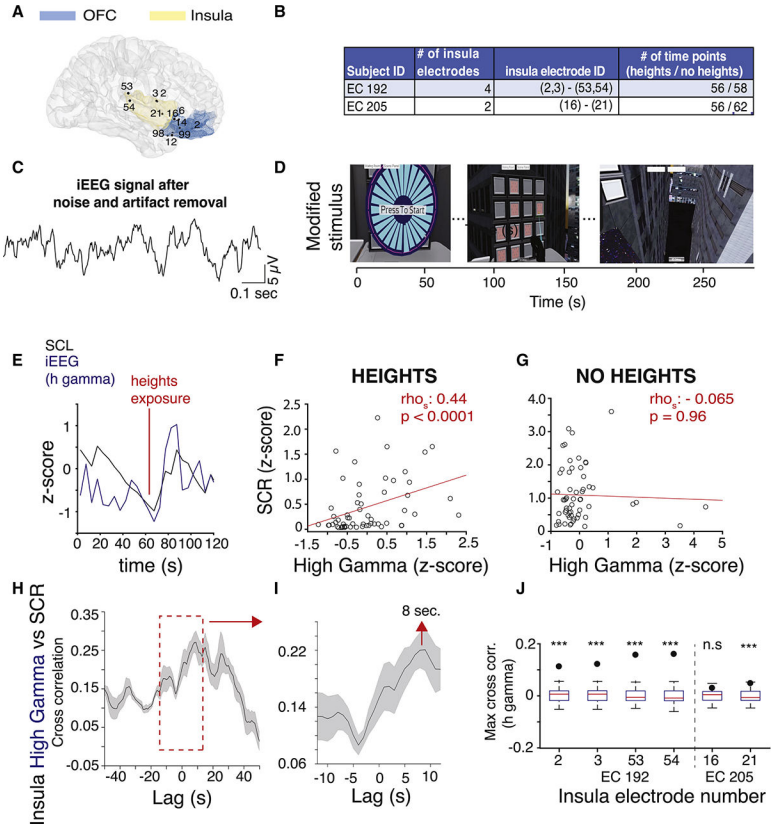

Figure 5. Modulation of Insula Activity during Visual Threat

(A) MRI reconstruction showing the location of the insula and OFC electrodes from patients EC 192, EC 200, and EC 205 (right hemisphere right view).

(B) Number and IDs of insula electrodes and number of time points during the heights and no heights stimuli recorded from each subject with insula electrodes. Electrodes in parentheses are on the same lead.

(C) Example iEEG signal from an insula electrode (ch 2) after line noise and motion artifact removal.

(D) Screen shots from the modified heights stimulus with timeline.

(E) Example SCL (black) and insula high gamma iEEG (blue) signals during heights exposure from 1 electrode (#2, EC 192).

(F) Scatterplot showing high gamma amplitude plotted against SCR during heights from 1 example electrode (ch 2, EC 192). Each dot represents a 5 s average of brain activity and SCR.

(G) Same as (D) during no heights.

(H) Cross-correlogram for SCR and insula high gamma activity. Dark line, mean correlation for each lag; shaded area, SEM.

(I) Zoom-in of the red inset in (H).

(J) Cross-correlation coefficients (dots) between SCR and high gamma activity and the distribution of permuted cross-correlation coefficients are plotted for each insula electrode in the boxplots. Edges of the box are 25th and 75th percentile. ***p < 0.0001; n.s, non-significant.

See also Figures S3–S5, Table S4, and Video S3.

A

Subject ID	# of OFC electrodes	OFC electrode IDs	# of time points (heights / no heights)
EC 200	2	(98, 99)	61 / 61
EC 205	5	(1, 2, 6) - (12,14)	56 / 62

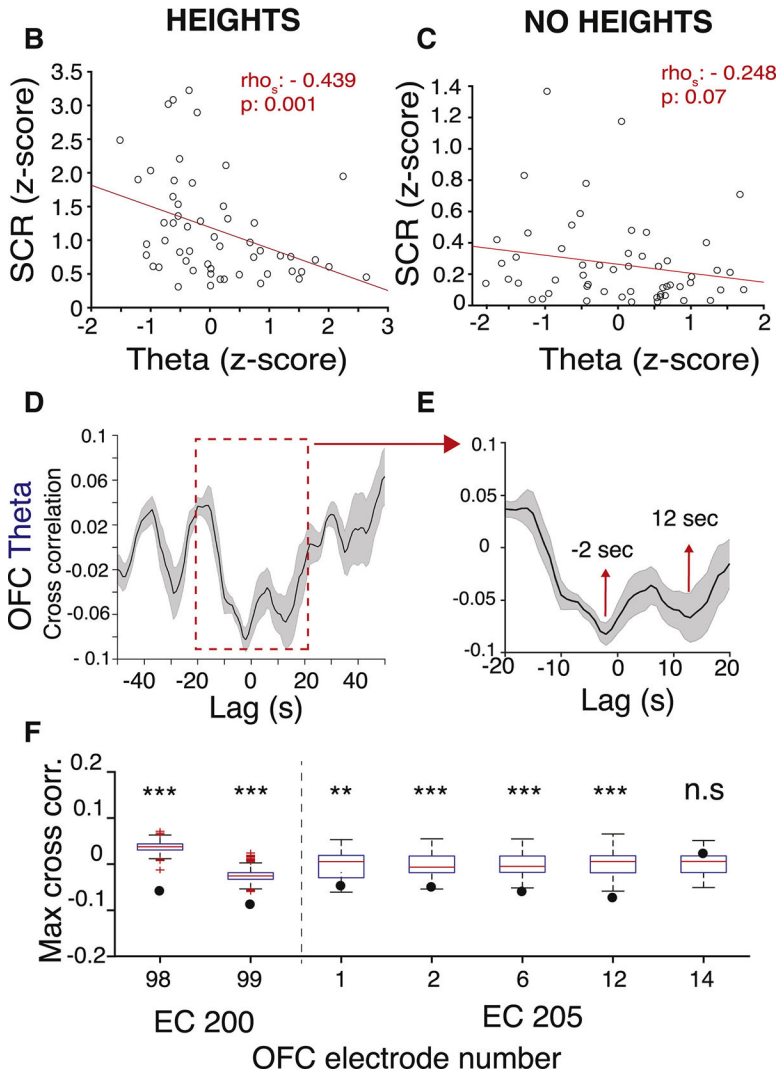

Figure 6. Modulation of OFC Activity during Visual Threat

(A) Number and IDs of OFC electrodes and number of time points during the heights and no heights stimuli recorded from each subject with OFC electrodes. Electrodes that are in the same parenthesis are located on the same lead.

(B) Scatterplot showing the correlation between theta in OFC and SCR during heights from example electrode #98, EC 200.

(C) Same as (A) during no heights. rho$_s$, Spearman correlation coefficient.

(D) Cross-correlogram for SCR and OFC theta activity. Dark line, mean correlation for each lag; shaded area, SEM.

(E) Zoom-in of the red inset in (C).

(F) Cross-correlation coefficients and the distribution of permuted cross-correlation coefficients are plotted for each OFC electrode. Edges of the box are 25^{th} and 75^{th} percentile. ***$p < 0.001$, **$p < 0.01$.

See also Figures S3 and S4, Table S4, and Video S3.

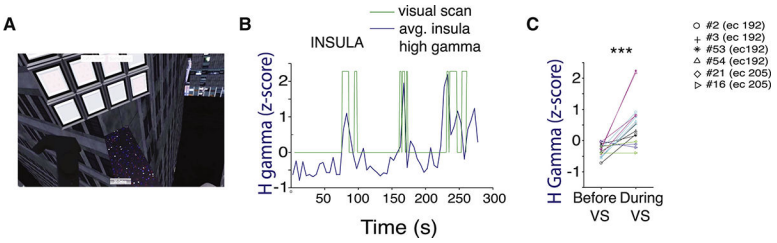

Figure 7. Modulation of Insula Activity during Visual Scanning in Virtual Heights

(A) A screenshot of a patient's view looking down at heights in VR.

(B) Insula high gamma amplitude during heights superimposed onto the visual scanning episodes taken from patient EC192, averaged across all electrodes.

(C) Normalized high gamma amplitude before and during each visual scan. Each color is a separate visual scan. Each marker represents a separate insula electrode.

See also Figure S5, Table S2, and Video S3.

KEY RESOURCES TABLE

REAGENT or RESOURCE	SOURCE	IDENTIFIER
Deposited Data		
Raw Data	This paper	https://doi.org/10.5061/dryad.wdbrv15mq
Software and Algorithms		
MATLAB	Mathworks (Natick, MA)	R2020b
FreeSurfer	[57]	https://surfer.nmr.mgh.harvard.edu
EDA processing scripts	[58]	https://github.com/lciti/cvxEDA
Custom processing scripts	This paper	https://doi.org/10.5061/dryad.wdbrv15mq
Unity V2017.3.03f	UnityTechnologies. This paper	https://stanfordmedicine.box.com/s/lrpc9accsh9i5sechznph5cx1hf793uh
HTC Vive	HTC Corporation	V 1.7.3
Steam VR	Valve Corporation	V 1.10.22
Acqknowledge	Biopac Systems	V 4.4
Tobii Pro Eye Tracking	Tobii AB	V 2.9.1